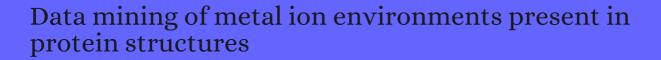
CITATION REPORT List of articles citing



DOI: 10.1016/j.jinorgbio.2008.05.006 Journal of Inorganic Biochemistry, 2008, 102, 1765-76.

Source: https://exaly.com/paper-pdf/43487439/citation-report.pdf

Version: 2024-04-28

This report has been generated based on the citations recorded by exaly.com for the above article. For the latest version of this publication list, visit the link given above.

The third column is the impact factor (IF) of the journal, and the fourth column is the number of citations of the article.

#	Paper	IF	Citations
254	Structural and functional analysis of AsbF: origin of the stealth 3,4-dihydroxybenzoic acid subunit for petrobactin biosynthesis. 2008 , 105, 17133-8		47
253	Benefits of structural genomics for drug discovery research. 2009 , 9, 459-74		23
252	Structure-based mechanism of lipoteichoic acid synthesis by Staphylococcus aureus LtaS. 2009 , 106, 1584-9		75
251	Copper binding to beta-2-microglobulin and its pre-amyloid oligomers. 2009 , 48, 9871-81		42
250	Crystal structures of mite allergens Der f 1 and Der p 1 reveal differences in surface-exposed residues that may influence antibody binding. <i>Journal of Molecular Biology</i> , 2009 , 386, 520-30	6.5	64
249	Crystal structures of A. acidocaldarius endoglucanase Cel9A in complex with cello-oligosaccharides: strong -1 and -2 subsites mimic cellobiohydrolase activity. <i>Journal of Molecular Biology</i> , 2009 , 394, 61-70	6.5	24
248	Factors governing metal-ligand distances and coordination geometries of metal complexes. 2009 , 113, 2952-60		88
247	Discovery of leukotriene A4 hydrolase inhibitors using metabolomics biased fragment crystallography. 2009 , 52, 4694-715		103
246	To automate or not to automate: this is the question. 2010 , 11, 211-21		23
245	Unmet challenges of structural genomics. 2010 , 20, 587-97		40
244	Amino acid influence on copper binding to peptides: cysteine versus arginine. 2010 , 21, 522-33		36
243	New surface contacts formed upon reductive lysine methylation: improving the probability of protein crystallization. <i>Protein Science</i> , 2010 , 19, 1395-404	6.3	24
242	New evidence for the role of calcium in the glycosidase reaction of GH43 arabinanases. 2010 , 277, 4562	-74	38
241	Trinuclear Metal Clusters in Catalysis by Terpenoid Synthases. 2010 , 82, 1585-1597		92
240	Metals in protein structures: a review of their principal features. 2010 , 16, 247-302		114
239	SHotSmacromolecular crystals. 2009, 10, 580		6
238	Crystal structure and molecular modeling study of N-carbamoylsarcosine amidase Ta0454 from Thermoplasma acidophilum. 2010 , 169, 304-11		13

(2012-2010)

237	sativum with a broad specificity for natural and synthetic aminoaldehydes. <i>Journal of Molecular Biology</i> , 2010 , 396, 870-82	6.5	44
236	Bioinformatics in bioinorganic chemistry. 2010 , 2, 39-51		16
235	Metalloproteomics, metalloproteomes, and the annotation of metalloproteins. 2010 , 2, 117-25		112
234	Stimulation of lignocellulosic biomass hydrolysis by proteins of glycoside hydrolase family 61: structure and function of a large, enigmatic family. 2010 , 49, 3305-16		597
233	Bacterial Surface Display of Metal-Binding Sites. 2011 , 249-283		2
232	Microbial Biosorption of Metals. 2011 ,		41
231	X-ray crystallography: Assessment and validation of protein-small molecule complexes for drug discovery. 2011 , 6, 771-782		46
230	A new generation of crystallographic validation tools for the protein data bank. 2011 , 19, 1395-412		335
229	Computational investigation of the histidine ammonia-lyase reaction: a modified loop conformation and the role of the zinc(II) ion. 2011 , 17, 1551-63		11
228	BrabA.11339.a: anomalous diffraction and ligand binding guide towards the elucidation of the function of a Sputative Elactamase-like proteinSfrom Brucella melitensis. 2011 , 67, 1106-12		4
227	Structure of a Nudix hydrolase (MutT) in the Mg(2+)-bound state from Bartonella henselae, the bacterium responsible for cat scratch fever. 2011 , 67, 1078-83		4
226	Structure of fumarate hydratase from Rickettsia prowazekii, the agent of typhus and suspected relative of the mitochondria. 2011 , 67, 1123-8		3
225	Monitoring and validating active site redox states in protein crystals. 2011 , 1814, 778-84		29
224	The crystal structure of the lipid II-degrading bacteriocin syringacin M suggests unexpected evolutionary relationships between colicin M-like bacteriocins. 2012 , 287, 38876-88		28
223	Analysis of copper-ligand bond lengths in X-ray structures of different types of copper sites in proteins. 2012 , 68, 1223-31		18
222	Pattern prediction and coordination geometry analysis from cadmium-binding proteins: a computational approach. 2012 , 68, 1346-58		17
221	Mining the Cambridge Structural Database for Bioisosteres. 2012 , 75-101		5
220	The crystal structure of human [41)-microglobulin reveals a potential haem-binding site. 2012, 445, 175-	82	25

219	How alkali metal ion binding alters the conformation preferences of gramicidin A: a molecular dynamics and ion mobility study. 2012 , 116, 689-96	27
218	Molecular determinants for antibody binding on group 1 house dust mite allergens. 2012 , 287, 7388-98	61
217	1.8 Structure Validation and Analysis. 2012 , 116-135	1
216	Crystal structures of putative phosphoglycerate kinases from B. anthracis and C. jejuni. 2012 , 13, 15-26	7
215	Structural and immunologic characterization of bovine, horse, and rabbit serum albumins. 2012 , 52, 174-82	600
214	Coordination sphere tuning of the electron transfer dissociation behavior of Cu(II)-peptide complexes. 2012 , 23, 321-9	15
213	A database of alkaline-earth-coordinated peptide cross sections: insight into general aspects of structure. 2013 , 24, 768-79	18
212	In-house zinc SAD phasing at Cu Kædge. 2013 , 36, 74-81	8
211	Heterometallic [AgFe(3)S (4)] ferredoxin variants: synthesis, characterization, and the first crystal structure of an engineered heterometallic iron-sulfur protein. 2013 , 18, 261-76	9
210	Regulation of actin by ion-linked equilibria. 2013 , 105, 2621-8	26
209	Zinc coordination spheres in protein structures. 2013 , 52, 10983-91	144
208	Cysteine dioxygenase structures from pH4 to 9: consistent cys-persulfenate formation at intermediate pH and a Cys-bound enzyme at higher pH. <i>Journal of Molecular Biology</i> , 2013 , 425, 3121-36 ^{6.5}	52
207	Crystallographic model validation: from diagnosis to healing. 2013 , 23, 707-14	12
206	Structural characterization of the RLCK family member BSK8: a pseudokinase with an unprecedented architecture. <i>Journal of Molecular Biology</i> , 2013 , 425, 4455-67	21
205	The binding of Ca2+, Co2+, Ni2+, Cu2+, and Zn2+ cations to angiotensin I determined by mass spectrometry based techniques. 2013 , 354-355, 318-325	17
204	Random coil structures in bacterial proteins. Relationships of their amino acid compositions to flanking structures and corresponding genic base compositions. 2013 , 95, 1745-54	14
203	Designing functional metalloproteins: from structural to catalytic metal sites. 2013 , 257, 2565-2588	96
202	Investigation of non-corrin cobalt(II)-containing sites in protein structures of the Protein Data Bank. 2013 , 69, 176-83	5

(2014-2013)

2	201	Controlled self-assembly of CdTe quantum dots into different microscale dendrite structures by using proteins as templates. 2013 , 1, 15082		6	
2	200	Molecular mechanisms of inhibition of influenza by surfactant protein D revealed by large-scale molecular dynamics simulation. 2013 , 52, 8527-38		28	
1	199	The TP0796 lipoprotein of Treponema pallidum is a bimetal-dependent FAD pyrophosphatase with a potential role in flavin homeostasis. 2013 , 288, 11106-21		21	
1	198	Plant ALDH10 family: identifying critical residues for substrate specificity and trapping a thiohemiacetal intermediate. 2013 , 288, 9491-507		30	
1	-97	Atomic model of the F420-reducing [NiFe] hydrogenase by electron cryo-microscopy using a direct electron detector. <i>ELife</i> , 2014 , 3, e01963	8.9	106	
1	196	Secondary structure preferences of mn (2+) binding sites in bacterial proteins. 2014 , 2014, 501841		8	
1	95	Apo, Zn2+-bound and Mn2+-bound structures reveal ligand-binding properties of SitA from the pathogen Staphylococcus pseudintermedius. 2014 , 34, e00154		26	
1	94	The future of crystallography in drug discovery. 2014 , 9, 125-37		51	
1	193	Structural analysis of human soluble adenylyl cyclase and crystal structures of its nucleotide complexes-implications for cyclase catalysis and evolution. 2014 , 281, 4151-64		22	
1	192	Continuous mutual improvement of macromolecular structure models in the PDB and of X-ray crystallographic software: the dual role of deposited experimental data. 2014 , 70, 2533-43		21	
1	191	Na+/K+ exchange switches the catalytic apparatus of potassium-dependent plant L-asparaginase. 2014 , 70, 1854-72		16	
1	190	The structure of the cysteine protease and lectin-like domains of Cwp84, a surface layer-associated protein from Clostridium difficile. 2014 , 70, 1983-93		13	
1	189	Zinc-selective inhibition of the promiscuous bacterial amide-hydrolase DapE: implications of metal heterogeneity for evolution and antibiotic drug design. 2014 , 6, 88-95		19	
1	288	Function-based assessment of structural similarity measurements using metal co-factor orientation. 2014 , 82, 648-56		12	
1	187	Unique effect of Cu(II) in the metal-induced amyloid formation of ⊞-microglobulin. 2014 , 53, 1263-74		15	
1	:86	Identifying Zn-bound histidine residues in metalloproteins using hydrogen-deuterium exchange mass spectrometry. 2014 , 86, 766-73		11	
1	185	Stimuli-sensitive intrinsically disordered protein brushes. 2014 , 5, 5145		51	
1	284	Automated identification of elemental ions in macromolecular crystal structures. 2014 , 70, 1104-14		27	

183	Radical SAM enzyme QueE defines a new minimal core fold and metal-dependent mechanism. 2014 , 10, 106-12		57
182	Analyses of cobalt-ligand and potassium-ligand bond lengths in metalloproteins: trends and patterns. 2014 , 20, 2271		2
181	Force field independent metal parameters using a nonbonded dummy model. 2014 , 118, 4351-62		110
180	In silico analysis of metal coordination geometry in arsenic, beryllium, and lead bound structures. 2014 , 67, 1888-1904		4
179	Designing hydrolytic zinc metalloenzymes. 2014 , 53, 957-78		94
178	Validation of metal-binding sites in macromolecular structures with the CheckMyMetal web server. 2014 , 9, 156-70		200
177	Structural basis for catalysis in a CDP-alcohol phosphotransferase. 2014 , 5, 4068		27
176	Structure of a prokaryotic sodium channel pore reveals essential gating elements and an outer ion binding site common to eukaryotic channels. <i>Journal of Molecular Biology</i> , 2014 , 426, 467-83	6.5	111
175	Evolution of plant [11)-pyrroline-5-carboxylate reductases from phylogenetic and structural perspectives. 2015 , 6, 567		16
174	Structural basis for the targeting of complement anaphylatoxin C5a using a mixed L-RNA/L-DNA aptamer. 2015 , 6, 6481		47
173	Magnesium-binding architectures in RNA crystal structures: validation, binding preferences, classification and motif detection. <i>Nucleic Acids Research</i> , 2015 , 43, 3789-801	20.1	63
172	Structural and biochemical characterization of a novel aminopeptidase from human intestine. 2015 , 290, 11321-36		8
171	How simple is too simple? Computational perspective on importance of second-shell environment for metal-ion selectivity. 2015 , 17, 14393-404		5
170	Biochemical and structural investigation of two paralogous glycoside hydrolases from Zobellia galactanivorans: novel insights into the evolution, dimerization plasticity and catalytic mechanism of the GH117 family. 2015 , 71, 209-23		16
169	Protein arginine deiminase 2 binds calcium in an ordered fashion: implications for inhibitor design. 2015 , 10, 1043-53		68
168	Computational methods for prediction of RNA interactions with metal ions and small organic ligands. 2015 , 553, 261-85		8
167	A control on hydrophobic and hydrophilic interactions between HEWL and metal Schiff-base complexes comprising of different metal ions and ligands. 2015 , 161, 54-62		3
166	Cwp84, a Clostridium difficile cysteine protease, exhibits conformational flexibility in the absence of its propeptide. 2015 , 71, 295-303		5

(2016-2015)

165	Crystal structure of a mirror-image L-RNA aptamer (Spiegelmer) in complex with the natural L-protein target CCL2. 2015 , 6, 6923		60
164	X-ray crystallography over the past decade for novel drug discovery - where are we heading next?. 2015 , 10, 975-89		38
163	Using support vector machines to improve elemental ion identification in macromolecular crystal structures. 2015 , 71, 1147-58		4
162	The copper binding properties of metforminQCM-D, XPS and nanobead agglomeration. 2015 , 51, 1731	3-6	18
161	Sperm Lysozyme-Like Protein 1 (SLLP1), an intra-acrosomal oolemmal-binding sperm protein, reveals filamentous organization in protein crystal form. 2015 , 3, 756-71		6
160	Structure of the ordered hydration of amino acids in proteins: analysis of crystal structures. 2015 , 71, 2192-202		19
159	Histidine phosphorylation relieves copper inhibition in the mammalian potassium channel KCa3.1. <i>ELife</i> , 2016 , 5,	8.9	37
158	Minimal Functional Sites in Metalloproteins and Their Usage in Structural Bioinformatics. <i>International Journal of Molecular Sciences</i> , 2016 , 17,	6.3	7
157	Structure of the host-recognition device of Staphylococcus aureus phage ?11. <i>Scientific Reports</i> , 2016 , 6, 27581	4.9	35
156	Crystal structure of Anoxybacillus \text{\text{\text{Bmylase} provides insights into maltose binding of a new glycosyl hydrolase subclass. <i>Scientific Reports</i> , 2016 , 6, 23126	4.9	27
155	X-ray structures and mechanism of the human serotonin transporter. 2016 , 532, 334-9		364
154	Binding of metals to purine N7 nitrogen atoms and implications for nucleic acids: A CSD survey. 2016 , 452, 82-89		20
153	Crystal Structure of the Neuropilin-1 MAM Domain: Completing the Neuropilin-1 Ectodomain Picture. 2016 , 24, 2008-2015		22
152	Structures of PspAG97A lglucoside hydrolase reveal a novel mechanism for chloride induced activation. 2016 , 196, 426-436		3
151	Conserved methionine dictates substrate preference in Nramp-family divalent metal transporters. 2016 , 113, 10310-5		51
150	New Mechanistic Insight from Substrate- and Product-Bound Structures of the Metal-Dependent Dimethylsulfoniopropionate Lyase DddQ. 2016 , 55, 6162-6174		20
149	Synthesis, X-ray Structures, Electronic Properties, and O/NO Reactivities of Thiol Dioxygenase Active-Site Models. 2016 , 55, 11839-11853		22
148	Elucidation of Lipid Binding Sites on Lung Surfactant Protein A Using X-ray Crystallography, Mutagenesis, and Molecular Dynamics Simulations. 2016 , 55, 3692-701		15

147	Sodium and Potassium Interactions with Nucleic Acids. 2016 , 16, 167-201		27
146	Metalloprotein Crystallography: More than a Structure. 2016 , 49, 695-702		45
145	Seedless, copper-induced synthesis of stable Ag/Cu bimetallic nanoparticles and their optical properties. 2016 , 6, 29116-29126		25
144	Safeguarding Structural Data Repositories against Bad Apples. 2016 , 24, 216-20		29
143	Atomic resolution probe for allostery in the regulatory thin filament. 2016 , 113, 3257-62		45
142	Structural analysis and unique molecular recognition properties of a Bauhinialforficata lectin that inhibits cancer cell growth. 2017 , 284, 429-450		19
141	Proteome scale identification, classification and structural analysis of iron-binding proteins in bread wheat. <i>Journal of Inorganic Biochemistry</i> , 2017 , 170, 63-74	4.2	7
140	Mg2+ ions: do they bind to nucleobase nitrogens?. <i>Nucleic Acids Research</i> , 2017 , 45, 987-1004	20.1	56
139	Identification and Characterization of a Secondary Sodium-Binding Site and the Main Selectivity Determinants in the Human Concentrative Nucleoside Transporter 3. 2017 , 14, 1980-1987		7
138	A Database of Transition-Metal-Coordinated Peptide Cross-Sections: Selective Interaction with Specific Amino Acid Residues. 2017 , 28, 1293-1303		7
137	Exploring cucurbit[6]urilpeptide interactions in the solid state: crystal structure of cucurbit[6]uril complexes with glycyl-containing dipeptides. 2017 , 19, 3892-3897		6
136	Structural and Biochemical Insights into Dimethylsulfoniopropionate Cleavage by Cofactor-Bound DddK from the Prolific Marine Bacterium Pelagibacter. 2017 , 56, 2873-2885		21
135	Structure of the ACF7 EF-Hand-GAR Module and Delineation of Microtubule Binding Determinants. 2017 , 25, 1130-1138.e6		11
134	Optimization of overexpression of a chaperone protein of steroid C25 dehydrogenase for biochemical and biophysical characterization. 2017 , 134, 47-62		4
133	Comparison of metal-binding strength between methionine and cysteine residues: Implications for the design of metal-binding motifs in proteins. 2017 , 224, 32-39		9
132	Data mining of iron(II) and iron(III) bond-valence parameters, and their relevance for macromolecular crystallography. <i>Acta Crystallographica Section D: Structural Biology</i> , 2017 , 73, 316-325	5.5	23
131	Meprin land BMP-1 are differentially regulated by CaCl. 2017 , 65, 8-13		5
130	Structure of the infectious salmon anemia virus receptor complex illustrates a unique binding strategy for attachment. 2017 , 114, E2929-E2936		10

129	Biased agonism and allosteric modulation of G protein-coupled receptor 183 - a 7TM receptor also known as Epstein-Barr virus-induced gene 2. 2017 , 174, 2031-2042		10
128	Rickettsia prowazekii methionine aminopeptidase as a promising target for the development of antibacterial agents. 2017 , 25, 813-824		5
127	Mechanisms of zinc binding to the solute-binding protein AztC and transfer from the metallochaperone AztD. 2017 , 292, 17496-17505		16
126	Crystal structure of glucose isomerase in complex with xylitol inhibitor in one metal binding mode. 2017 , 493, 666-670		11
125	Structural basis for IL-1#ecognition by a modified DNA aptamer that specifically inhibits IL-1# signaling. 2017 , 8, 810		40
124	New Evidence for the Mechanism of Action of a Type-2 Diabetes Drug Using a Magnetic Bead-Based Automated Biosensing Platform. 2017 , 2, 1329-1336		7
123	Monovalent Cation Activation of the Radical SAM Enzyme Pyruvate Formate-Lyase Activating Enzyme. 2017 , 139, 11803-11813		18
122	Transition metal binding selectivity in proteins and its correlation with the phylogenomic classification of the cation diffusion facilitator protein family. <i>Scientific Reports</i> , 2017 , 7, 16381	4.9	54
121	Metal ion - Dehydrin interactions investigated by affinity capillary electrophoresis and computer models. 2017 , 216, 219-228		11
120	Conformational flexibility of PL12 family heparinases: structure and substrate specificity of heparinase III from Bacteroides thetaiotaomicron (BT4657). 2017 , 27, 176-187		10
119	Activity inhibition and crystal polymorphism induced by active-site metal swapping. <i>Acta Crystallographica Section D: Structural Biology</i> , 2017 , 73, 641-649	5.5	5
118	Crystal Structure of Colocasia esculenta Tuber Agglutinin at 1.74 Resolution and Its Quaternary Interactions. 2017 , 06,		1
117	Characterizing metal-binding sites in proteins with X-ray crystallography. 2018, 13, 1062-1090		47
116	Thermal and chemical denaturation of Colocasia esculenta tuber agglutinin from to unfolded state. 2018 , 36, 2179-2193		
115	In Silico Studies of Mammalian EALAD Interactions with Selenides and Selenoxides. 2018 , 37, e1700091		6
114	Molstack-Interactive visualization tool for presentation, interpretation, and validation of macromolecules and electron density maps. <i>Protein Science</i> , 2018 , 27, 86-94	6.3	25
113	Unintentional Genomic Changes Endow with an Augmented Heavy-Metal Resistance. 2018, 9,		6
112	Metal-Assisted Assembly of Protein Containers Loaded with Inorganic Nanoparticles. 2018 , 57, 13431-1	3436	9

111	Identification of a unique Ca-binding site in rat acid-sensing ion channel 3. 2018 , 9, 2082		11
110	Understanding the Interplay between Self-Assembling Peptides and Solution Ions for Tunable Protein Nanoparticle Formation. 2018 , 12, 6956-6967		12
109	Ig-like Domain in Endoglucanase Cel9A from Alicyclobacillus acidocaldarius Makes Dependent the Enzyme Stability on Calcium. 2018 , 60, 698-711		4
108	Structural studies of the unusual metal-ion site of the GH124 endoglucanase from Ruminiclostridium thermocellum. 2018 , 74, 496-505		1
107	Structural features of uranium-protein complexes. <i>Journal of Inorganic Biochemistry</i> , 2018 , 189, 1-6	4.2	8
106	PlaneFinder: a methodology to find the best plane for a set of atoms involved in the metal coordination in protein structures. 2018 , 51, 1251-1256		
105	Structural Basis of Homology-Directed DNA Repair Mediated by RAD52. 2018 , 3, 50-62		21
104	Calcium is an essential cofactor for metal efflux by the ferroportin transporter family. 2018 , 9, 3075		26
103	Structural analysis of substrate recognition by glucose isomerase in Mn binding mode at M2 site in S.Irubiginosus. 2018 , 503, 770-775		15
102	Evolution of chemokine receptors is driven by mutations in the sodium binding site. <i>PLoS Computational Biology</i> , 2018 , 14, e1006209	5	13
101	Metal Coordination Is Crucial for Geranylgeranyl Diphosphate Synthase-Bisphosphonate Interactions: A Crystallographic and Computational Analysis. 2019 , 96, 580-588		3
100	Insights into an unusual Auxiliary Activity 9 family member lacking the histidine brace motif of lytic polysaccharide monooxygenases. 2019 , 294, 17117-17130		19
99	Conformation and Domain Movement Analysis of Human Matrix Metalloproteinase-2: Role of Associated Zn and Ca Ions. <i>International Journal of Molecular Sciences</i> , 2019 , 20,	6.3	2
98	FtsW is a peptidoglycan polymerase that is functional only in complex with its cognate penicillin-binding protein. 2019 , 4, 587-594		143
97	Structural and biochemical analysis of a phosin from Streptomyces chartreusis reveals a combined polyphosphate- and metal-binding fold. 2019 , 593, 2019-2029		7
96	The Axonal Motor Neuropathy-Related HINT1 Protein Is a Zinc- and Calmodulin-Regulated Cysteine SUMO Protease. 2019 , 31, 503-520		5
95	Bioinspired Histidine?Zn Coordination for Tuning the Mechanical Properties of Self-Healing Coiled Coil Cross-Linked Hydrogels. 2019 , 4,		15
94	Structural analyses of NudT16-ADP-ribose complexes direct rational design of mutants with improved processing of poly(ADP-ribosyl)ated proteins. <i>Scientific Reports</i> , 2019 , 9, 5940	4.9	8

93	Data mining new energy materials from structure databases. 2019 , 107, 554-567		19
92	Artificial Neural Networks for Prediction of Tuberculosis Disease. 2019 , 10, 395		22
91	Crystal structures of thiamine monophosphate kinase from Acinetobacter baumannii in complex with substrates and products. <i>Scientific Reports</i> , 2019 , 9, 4392	.9	1
90	ZincBind-the database of zinc binding sites. 2019 , 2019,		20
89	Comparative Analysis of Protein Hydration from MD simulations with Additive and Polarizable Force Fields. 2019 , 2, 1800106		16
88	Structural knowledge or X-ray damage? A case study on xylose isomerase illustrating both. 2019 , 26, 931-944		6
87	Enzymatic synthesis of l-fucose from l-fuculose using a fucose isomerase from sp. and the biochemical and structural analyses of the enzyme. 2019 , 12, 282		7
86	Mutation of two key aspartate residues alters stoichiometry of the NhaB Na/H exchanger from Klebsiella pneumoniae. <i>Scientific Reports</i> , 2019 , 9, 15390	.9	1
85	Nucleobase carbonyl groups are poor Mg inner-sphere binders but excellent monovalent ion binders-a critical PDB survey. 2019 , 25, 173-192		18
84	Aspergillus oryzae S2 AmyA amylase expression in Pichia pastoris: production, purification and novel properties. 2019 , 46, 921-932		6
83	Structural and functional characterization of an intradiol ring-cleavage dioxygenase from the polyphagous spider mite herbivore Tetranychus urticae Koch. 2019 , 107, 19-30		3
82	Mining the Enriched Subgraphs for Specific Vertices in a Biological Graph. 2019 , 16, 1496-1507		1
81	Structural dynamics behind variants in pyrazinamidase and pyrazinamide resistance. 2020 , 38, 3003-3017		4
80	Spectrometric, Thermodynamic, pH Metric and Viscometric Studies on the Binding of TEALS as Surfactant with Albumin as Biopolymer. <i>Current Physical Chemistry</i> , 2020 , 10, 47-64	.5	O
79	In Vivo Metal Catalysis in Living Biological Systems. 2020 , 309-353		4
78	High-Throughput PIXE as an Essential Quantitative Assay for Accurate Metalloprotein Structural Analysis: Development and Application. 2020 , 142, 185-197		10
77	The Effects of the Metal Ion Substitution into the Active Site of Metalloenzymes: A Theoretical Insight on Some Selected Cases. 2020 , 10, 1038		10
76	Metal ions shape ⊞ynuclein. <i>Scientific Reports</i> , 2020 , 10, 16293 4.	.9	18

75	vsFilt: A Tool to Improve Virtual Screening by Structural Filtration of Docking Poses. <i>Journal of Chemical Information and Modeling</i> , 2020 , 60, 3692-3696	7
74	The coupling mechanism of mammalian respiratory complex I. 2020 , 370,	58
73	Benchmarking polarizable and non-polarizable force fields for Ca-peptides against a comprehensive QM dataset. <i>Journal of Chemical Physics</i> , 2020 , 153, 144102	5
72	Femtosecond-to-millisecond structural changes in a light-driven sodium pump. 2020 , 583, 314-318	48
71	Protein Design for the Synthesis and Stabilization of Highly Fluorescent Quantum Dots. 2020 , 32, 5729-5738	3 ₇
70	Intracellular Reactions Promoted by Bis(histidine) Miniproteins Stapled Using Palladium(II) Complexes. 2020 , 59, 9149-9154	37
69	Protein-ligand binding residue prediction enhancement through hybrid deep heterogeneous learning of sequence and structure data. 2020 , 36, 3018-3027	7
68	Investigation of manganese metal coordination in proteins: a comprehensive PDB analysis and quantum mechanical study. 2020 , 31, 1057-1064	4
67	Assessment of Crystallographic Structure Quality and ProteinLigand Complex Structure Validation. 2020 , 253-275	2
66	Intracellular Reactions Promoted by Bis(histidine) Miniproteins Stapled Using Palladium(II) Complexes. 2020 , 132, 9234-9239	16
65	Functional Distinction between Human and Mouse Sodium-Coupled Citrate Transporters and Its Biologic Significance: An Attempt for Structural Basis Using a Homology Modeling Approach. 2021 , 121, 5359-5377	7
64	The structure of human dermatan sulfate epimerase 1 emphasizes the importance of C5-epimerization of glucuronic acid in higher organisms. 2021 , 12, 1869-1885	1
63	Nucleobindin-2 consists of two structural components: The Zn-sensitive N-terminal half, consisting of nesfatin-1 and -2, and the Ca-sensitive C-terminal half, consisting of nesfatin-3. 2021 , 19, 4300-4318	O
62	Computational Structure Prediction Provides a Plausible Mechanism for Electron Transfer by the Outer Membrane Protein Cyc2 from Acidithiobacillus ferrooxidans.	
61	Identification of metal binding motifs in protein frameworks to develop novel remediation strategies for Hg and Cr(VI). 2021 , 34, 621-638	1
60	Rational design of metal-binding sites in domain-swapped myoglobin dimers. <i>Journal of Inorganic Biochemistry</i> , 2021 , 217, 111374	1
59	Structure of Escherichia coli respiratory complex I reconstituted into lipid nanodiscs reveals an uncoupled conformation.	1
58	Probing the Catalytic Mechanism and Inhibition of SAMHD1 Using the Differential Properties of Rand S-dNTP5 Diastereomers. 2021 , 60, 1682-1698	1

57	Computational structure prediction provides a plausible mechanism for electron transfer by the outer membrane protein Cyc2 from Acidithiobacillus ferrooxidans. <i>Protein Science</i> , 2021 , 30, 1640-1652	6.3	3
56	Working Mechanisms and Design Principles of Comb-like Polycarboxylate Ether Superplasticizers in Cement Hydration: Quantitative Insights for a Series of Well-Defined Copolymers. 2021 , 9, 8354-8371		6
55	Metal effect on intein splicing: A review. 2021 , 185, 53-67		3
54	IonoBiology: The functional dynamics of the intracellular metallome, with lessons from bacteria. <i>Cell Systems</i> , 2021 , 12, 497-508	10.6	3
53	Characterization of the substrate binding site of an iron detoxifying membrane transporter from Plasmodium falciparum. <i>Malaria Journal</i> , 2021 , 20, 295	3.6	0
52	Molecular dynamics study on the stability of foot-and-mouth disease virus particle in salt solution. <i>Molecular Simulation</i> , 2021 , 47, 1104-1111	2	О
51	Fabrication of a Fluorophore/Liquid-Crystal-Based Oligopeptide Biosensor for the Detection of Cu (II) Ions. <i>ChemistrySelect</i> , 2021 , 6, 6607-6618	1.8	3
50	Structure of respiratory complex I reconstituted into lipid nanodiscs reveals an uncoupled conformation. <i>ELife</i> , 2021 , 10,	8.9	8
49	Structural Insights into the Mechanism of Base Excision by MBD4. <i>Journal of Molecular Biology</i> , 2021 , 433, 167097	6.5	2
48	Cesium based phasing of macromolecules: a general easy to use approach for solving the phase problem. <i>Scientific Reports</i> , 2021 , 11, 17038	4.9	
47	A phosphate binding pocket is a key determinant of exo- versus endo-nucleolytic activity in the SNM1 nuclease family. <i>Nucleic Acids Research</i> , 2021 , 49, 9294-9309	20.1	1
46	Structural Contour Map of the Iota Carbonic Anhydrase from the Diatom Using a Multiprong Approach. <i>International Journal of Molecular Sciences</i> , 2021 , 22,	6.3	2
45	virusMED: an atlas of hotspots of viral proteins. <i>IUCrJ</i> , 2021 , 8,	4.7	2
44	Automated machine learning for endemic active tuberculosis prediction from multiplex serological data. <i>Scientific Reports</i> , 2021 , 11, 17900	4.9	1
43	InterMetalDB: A Database and Browser of Intermolecular Metal Binding Sites in Macromolecules with Structural Information. <i>Journal of Proteome Research</i> , 2021 , 20, 1889-1901	5.6	4
42	Beneficent and Maleficent Effects of Cations on Bufadienolide Binding to Na,K-ATPase. <i>Journal of Chemical Information and Modeling</i> , 2021 , 61, 976-986	6.1	2
41	Data management in the modern structural biology and biomedical research environment. <i>Methods in Molecular Biology</i> , 2014 , 1140, 1-25	1.4	25
40	Databases, Repositories, and Other Data Resources in Structural Biology. <i>Methods in Molecular Biology</i> , 2017 , 1607, 643-665	1.4	4

39	Conserved histidine residues at the ferroxidase centre of the Campylobacter jejuni Dps protein are not strictly required for metal binding and oxidation. <i>Microbiology (United Kingdom)</i> , 2016 , 162, 156-16	3 ^{2.9}	3
38	CheckMyMetal: a macromolecular metal-binding validation tool. <i>Acta Crystallographica Section D: Structural Biology</i> , 2017 , 73, 223-233	5.5	172
37	Crystal structure of Streptococcus pyogenes Csn2 reveals calcium-dependent conformational changes in its tertiary and quaternary structure. <i>PLoS ONE</i> , 2012 , 7, e33401	3.7	26
36	Ab initio coordination chemistry for nickel chelation motifs. <i>PLoS ONE</i> , 2015 , 10, e0126787	3.7	15
35	Structural and functional insights into the catalytic state of Cas9 HNH nuclease domain. <i>ELife</i> , 2019 , 8,	8.9	8
34	Activation of a nucleotide-dependent RCK domain requires binding of a cation cofactor to a conserved site. <i>ELife</i> , 2019 , 8,	8.9	6
33	Structure and mechanism of the Mrp complex, an ancient cation/proton antiporter. ELife, 2020, 9,	8.9	17
32	Protein Three-Dimensional Structure Validation. 2013,		
31	Identification of a Highly Conserved Hypothetical Protein TON_0340 as a Probable Manganese-Dependent Phosphatase. <i>PLoS ONE</i> , 2016 , 11, e0167549	3.7	
30	Transition metal binding selectivity in proteins and its correlation with the phylogenomic classification of the cation diffusion facilitator protein family.		O
29	Structural and functional characterization of CMP-N-acetylneuraminate synthetase from Vibrio cholerae. <i>Acta Crystallographica Section D: Structural Biology</i> , 2019 , 75, 564-577	5.5	
28	The Binding and Viscometric Studies of Ni+2, Co+2 and Mn+2 lons with Protein by Spectrometric and pH Metric Techniques. <i>Current Physical Chemistry</i> , 2019 , 9, 151-162	0.5	
27	Investigation of non-corrin cobalt(II)-containing sites in protein structures of the Protein Data Bank. <i>Acta Crystallographica Section B: Structural Science</i> , 2013 , 69, 176-183		
26	Beneficent and maleficent effects of cations on bufadienolide binding to Na+,K+-ATPase.		
25	Identification of Iron-Sulfur (Fe-S) Cluster and Zinc (Zn) Binding Sites Within Proteomes Predicted by DeepMinds AlphaFold2 Program Dramatically Expands the Metalloproteome. <i>Journal of Molecular Biology</i> , 2021 , 434, 167377	6.5	5
24	Determining the oxidation state of elements by X-ray crystallography <i>Acta Crystallographica Section D: Structural Biology</i> , 2022 , 78, 238-247	5.5	О
23	The oxytocin signaling complex reveals a molecular switch for cation dependence <i>Nature Structural and Molecular Biology</i> , 2022 ,	17.6	4
22	Druggability of Voltage-Gated Sodium Channels-Exploring Old and New Drug Receptor Sites		

21 fingeRNAt - a novel tool for high-throughput analysis of nucleic acid-ligand interactions.

20	Reorganization free energy of copper proteins in solution, in vacuum, and on metal surfaces <i>Journal of Chemical Physics</i> , 2022 , 156, 175101	3.9	2
19	fingeRNAtA novel tool for high-throughput analysis of nucleic acid-ligand interactions. <i>PLoS Computational Biology</i> , 2022 , 18, e1009783	5	1
18	Ca 2+ attenuates nucleation activity of leiomodin. <i>Protein Science</i> , 2022 , 31,	6.3	
17	Structural features stabilized by divalent cation coordination within hepatitis E virus ORF1 are critical for viral replication.		
16	Learning to Identify Physiological and Adventitious Metal-Binding Sites in the Three-Dimensional Structures of Proteins by Following the Hints of a Deep Neural Network. <i>Journal of Chemical Information and Modeling</i> , 2022 , 62, 2951-2960	6.1	О
15	Structural basis for lipid and copper regulation of the ABC transporter MsbA.		
14	Microbial Rhodopsins. 2022 , 1-52		1
13	The dimerized pentraxin-like domain of the adhesion G protein-coupled receptor 112 (ADGRG4) suggests function in sensing mechanical forces.		О
12	Biochemical studies highlight determinants for metal selectivity in the Escherichia coli periplasmic solute binding protein NikA.		O
11	Comparative homology of Pleurotus ostreatus laccase enzyme: Swiss model or Modeller?. 1-14		О
10	Structural basis for lipid and copper regulation of the ABC transporter MsbA. 2022 , 13,		О
9	CMM An enhanced platform for interactive validation of metal binding sites. 2023, 32,		1
8	Insights into divalent cation regulation and G13-coupling of orphan receptor GPR35. 2022, 8,		O
7	Geranylgeranyl diphosphate synthase: Role in human health, disease and potential therapeutic target. 2023 , 13,		O
6	Two independent loss-of-function mutations in anthocyanidin synthase homeologous genes are responsible for the all-green phenotype of sweet basil. 2023 , 175,		O
5	Why is manganese so valuable to bacterial pathogens?. 13,		О
4	Structural features stabilized by divalent cation coordination within hepatitis E virus ORF1 are critical for viral replication. 12,		1

3 Continuous Validation Across Macromolecular Structure Determination Process. **2023**, 65, 10-16 o

Study on Lowering the Group 1 Protease Allergens from House Dust Mites by Exposing to
Todomatsu Oil Atmosphere. **2023**, 14, 548

Contribution of calcium ligands in substrate binding and product release in the Acetovibrio thermocellus glycoside hydrolase family 9 cellulase CelR. **2023**, 299, 104655

О